Role of lubricin and boundary lubrication in the prevention of chondrocyte apoptosis

Kimberly A. Waller [a], Ling X. Zhang [b], Khaled A. Elsaid [c], Braden C. Fleming [a,d,e], Matthew L. Warman [f,g], and Gregory D. Jay [a,b,h,1]

[a]Center for Biomedical Engineering and the School of Engineering, Brown University, Providence, RI 02912; [b]Emergency Medicine Research Laboratory, Department of Emergency Medicine, Rhode Island Hospital, Providence, RI 02903; [d]Bioengineering Laboratory, Department of Orthopaedics, Alpert Medical School of Brown University and [e]Rhode Island Hospital, Providence, RI 02903; [c]Department of Pharmaceutical Sciences, Massachusetts College of Pharmacy and Health Sciences, Boston, MA 02115; [f]Orthopaedic Research Laboratories, Department of Orthopaedic Surgery, and [g]Howard Hughes Medical Institute, Boston Children's Hospital, Boston, MA 02115; and [h]Department of Emergency Medicine, Alpert Medical School of Brown University, Providence, RI 02903

Osteoarthritis is a complex disease involving the mechanical breakdown of articular cartilage in the presence of altered joint mechanics and chondrocyte death, but the connection between these factors is not well established. Lubricin, a mucinous glycoprotein encoded by the *PRG4* gene, provides boundary lubrication in articular joints. Joint friction is elevated and accompanied by accelerated cartilage damage in humans and mice that have genetic deficiency of lubricin. Here, we investigated the relationship between coefficient of friction and chondrocyte death using ex vivo and in vitro measurements of friction and apoptosis. We observed increases in whole-joint friction and cellular apoptosis in lubricin knockout mice compared with wild-type mice. When we used an in vitro bovine explant cartilage-on-cartilage bearing system, we observed a direct correlation between coefficient of friction and chondrocyte apoptosis in the superficial layers of cartilage. In the bovine explant system, the addition of lubricin as a test lubricant significantly lowered the static coefficient of friction and number of apoptotic chondrocytes. These results demonstrate a direct connection between lubricin, boundary lubrication, and cell survival and suggest that supplementation of synovial fluid with lubricin may be an effective treatment to prevent cartilage deterioration in patients with genetic or acquired deficiency of lubricin.

camptodactyly–arthropathy–coxa vara–pericarditis | shear strain | antiadhesion | tribology

Osteoarthritis (OA), which involves the degeneration of articular cartilage, is a prevalent disease with large societal and health care implications. Besides total joint replacement, there are no disease-modifying treatments for OA (1). Therefore, the identification of factors that can initiate OA is an area of extensive research. One hypothesis is that OA begins following an increase in coefficient of friction (COF) due to loss of boundary lubricant in synovial fluid (SF) (2). According to this hypothesis, increased friction between cartilage surfaces causes an increase in shear stress at the cartilage surface, which then affects chondrocyte metabolic function and survival. Ultimately, the combination of increased friction, loss of proteoglycan within the cartilage matrix, and chondrocyte death progresses to end-stage OA, characterized by full-thickness cartilage loss (3–5). Support for this hypothesis derives from studies demonstrating the critical role of chondrocytes in maintaining the articular cartilage matrix (6, 7) and associating chondrocyte apoptosis with OA pathology (8–10). However, a direct connection between friction and chondrocyte apoptosis has not yet been demonstrated in the context of lubricating SF components.

Cartilage lubrication in articulating joints is facilitated by SF, which contains the lubricating factors lubricin and hyaluronic acid (11–13). Lubricin, a mucinous glycoprotein produced by synovial cells and superficial zone chondrocytes (11, 14), provides lubrication in the boundary mode (15). Boundary lubrication dominates during periods of high load and low velocity,

when the lubricant film layer is thinner than the surface roughness (16). In healthy articular joints, a layer of lubricin molecules covers the surface of cartilage and acts as an antiadhesive and boundary lubricant to prevent cartilage damage as surface asperities move against each other (17–20). Patients with the autosomal recessive disease camptodactyly–arthropathy–coxa vara–pericarditis syndrome (CACP) lack functional lubricin and develop precocious cartilage failure. This disease has been recapitulated in mice in which the lubricin encoding gene, *Prg4*, has been knocked out. Early cartilage changes in mice lacking lubricin include fibrillation at the cartilage surface and loss of superficial zone chondrocytes (14, 21).

To determine whether increased friction is associated with loss of superficial zone chondrocytes, we measured whole-joint friction and observed the presence of apoptotic chondrocytes in tibiofemoral joints from lubricin knockout ($Prg4^{-/-}$), heterozygous ($Prg4^{+/-}$), and wild-type ($Prg4^{+/+}$) mice. We further investigated the role of lubricin using an in vitro bovine cartilage disk-on-disk bearing system. We lubricated this system with biologically relevant test solutions [e.g., normal human synovial fluid (HSF), SF from patients with CACP, lubricin purified from human synoviocyte culture] and measured friction and numbers of apoptotic chondrocytes. Herein, we show that friction and chondrocyte apoptosis are directly correlated, and both are reduced in the presence of lubricin.

Results

Chondrocyte Apoptosis in Mice with Different *Prg4* Genotypes. We stained coronal sections of knees from 10-wk-old $Prg4^{-/-}$, $Prg4^{+/-}$, and $Prg4^{+/+}$ mice for active caspase-3, which indicates cells in the execution stage of apoptosis (Fig. 1A). There were more chondrocytes with active caspase-3 in $Prg4^{-/-}$ knees compared with $Prg4^{+/+}$ and $Prg4^{+/-}$ knees. We also performed terminal deoxynucleotidyltransferase-mediated dUTP nick end labeling (TUNEL), as a second means of measuring programmed cell death in knees from mice with different *Prg4* genotypes. There were more TUNEL-positive cells in $Prg4^{-/-}$ knees compared with $Prg4^{+/+}$ and $Prg4^{+/-}$ knees (Fig. 1A). Regions of apoptotic chondrocytes in $Prg4^{-/-}$ knees were most pronounced in the upper middle zone just below the layer of flattened chondrocytes (Fig. 1A).

Whole-Joint COF in Mice with Different *Prg4* Genotypes. We measured whole-joint COF, which is manifested by contributions of
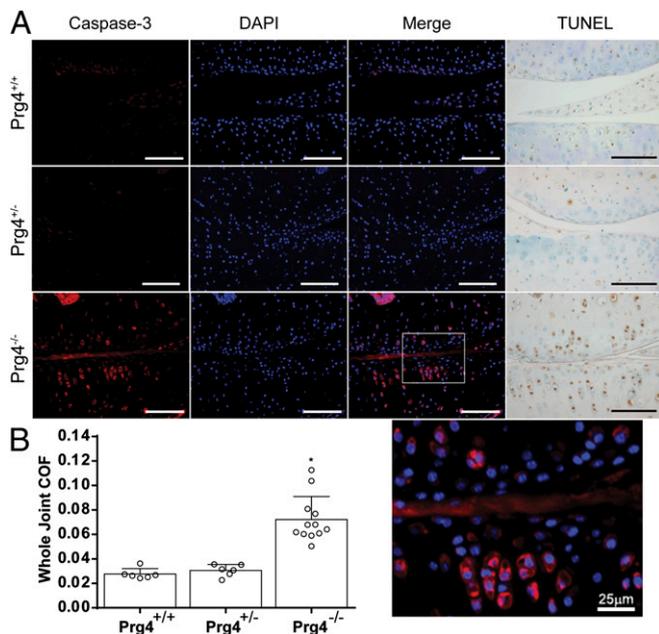
Fig. 1. (*A*) Chondrocyte apoptosis in mice with different *Prg4* genotypes. Activated caspase-3 immunodetection in coronal sections of knee joints from 10-wk-old wild-type (*Prg4$^{+/+}$*), heterozygous lubricin knockout (*Prg4$^{+/-}$*), and homozygous lubricin knockout (*Prg4$^{-/-}$*) mice that were not tested using the passive pendulum system. First column, Immunofluoresence detection (red) of active caspase-3. Second column, Same sections fluorescently imaged to reveal DAPI-stained (blue) chondrocyte nuclei. Third column, Merged active caspase-3 and DAPI images. Note the red fluorescence at the cartilage surface represents nonspecific antibody binding to proteinacious deposits that normally accumulate on the cartilage surface in *Prg4$^{-/-}$* mice. In contrast, the punctate red fluorescence observed below the cartilage surface overlaps with DAPI-stained nuclei indicating chondrocytes undergoing apoptosis. In contrast to *Prg4$^{-/-}$* knees, the knees in *Prg4$^{+/+}$* and *Prg4$^{+/-}$* mice had few chondrocytes with activated caspase-3. Fourth column, TUNEL staining and methyl green counterstaining of cartilage. More apoptotic (brown) chondrocyte nuclei are present in *Prg4$^{-/-}$* cartilage compared with *Prg4$^{+/+}$* and *Prg4$^{+/-}$* cartilage. (Scale bars, 100 μm.) (Bottom row) Region of interest taken from the image above to show the cells located just below the flattened superficial chondrocytes that are most susceptible to apoptosis. (*B*) Whole-joint COF in mice with different *Prg4* genotypes. Bar graphs depicting mean + 1 SD COF measurements in knee joints from 10-wk-old wild-type (*Prg4$^{+/+}$*), heterozygous lubricin knockout (*Prg4$^{+/-}$*), and homozygous lubricin knockout (*Prg4$^{-/-}$*) mice. Each individual COF measurement is indicated by an open circle. *Prg4$^{-/-}$* knees have significantly higher COF than either *Prg4$^{+/+}$* or *Prg4$^{+/-}$* knees. *$P < 0.01$ compared with *Prg4$^{+/+}$* or *Prg4$^{+/-}$* knees.

static and dynamic COF, using a passive pendulum system (22) in mouse knees from 10-wk-old *Prg4$^{-/-}$*, *Prg4$^{+/-}$*, and *Prg4$^{+/+}$* mice. The mean ± SD COF in *Prg4$^{-/-}$* knees was 0.072 ± 0.02 (*n* = 12 limbs), which was more than double that of *Prg4$^{+/+}$* (0.028 ± 0.004, *N* = 6 limbs, *P* = 0.0006) and *Prg4$^{+/-}$* (0.031 ± 0.005, *n* = 6 limbs, *P* = 0.0066) knees (Fig. 1*B*).

COF in Bovine Cartilage Bearings Lubricated with Different Test Solutions. We previously described a full-thickness bovine cartilage disk-on-disk bearing system for measuring static and kinetic COF in cartilage explants containing living chondrocytes (23). We lubricated this bearing system with five different test solutions: PBS, wild-type HSF, purified human synoviocyte lubricin in distilled water (HSL), HSF from patients with CACP (CACP-SF), and SF from patients with CACP to which purified human lubricin has been added (CACP-SF+HSL). CACP-SF is void of lubricin but otherwise contains normal SF components (24). The effects of these different test solutions on static and kinetic COF are depicted in Fig. 2.

The highest static COF measurements were observed in bearings tested with PBS as a lubricant. Lubricating bearings with CACP-SF did not reduce static COF compared with PBS, whereas significant reductions in COF were observed when bearings were lubricated with HSF, HSL, or CACP-SF+HSL. Comparing static COF between the lubricants HSL and CACP+HSL, enables us to investigate whether lubricin synergizes with other SF components, such as hyaluronic acid, to lower friction. We found no difference in static COF between these two lubricants, indicating that lubricin does not require other SF components to reduce static COF (12, 25) (Fig. 2).

Different results were obtained when kinetic COF was measured. The highest kinetic COF was obtained with PBS. All other test solutions (i.e., HSF, HSL, CACP-SF, and CACP-SF+HSL) were able to significantly reduce kinetic COF compared with PBS (Fig. 2). However, the greatest reductions in kinetic COF were achieved with HSF and CACP-SF+HSF (Fig. 2), which is consistent with lubricin and other SF components acting synergistically to lower kinetic COF.

Chondrocyte Apoptosis in Bovine Cartilage Bearings Lubricated with Different Test Solutions. After the cartilage bearings were lubricated with test solution and subjected to a friction and wear regimen, we processed the bearings to look for apoptotic cells by staining for active caspase-3 (Fig. 3). Many more chondrocytes in the bearings lubricated with PBS and CACP-SF contained active caspase-3 compared with chondrocytes in the bearings lubricated with HSF, HSL, and CACP-SF+HSL, or compared with bearings that were not subjected to load (i.e., unloaded controls). In bearings that were not lubricated with lubricin, cells located just below the flattened cells at the surface of cartilage appeared to be at highest risk for apoptosis (Fig. 3).

We quantified the percentage of apoptotic chondrocytes in three 100-μm-deep layers extending radially from the cartilage surface (Fig. 4*A*). The top layer contains superficial zone chondrocytes and some intermediate zone chondrocytes, whereas the next two layers contain intermediate zone chondrocytes (23).
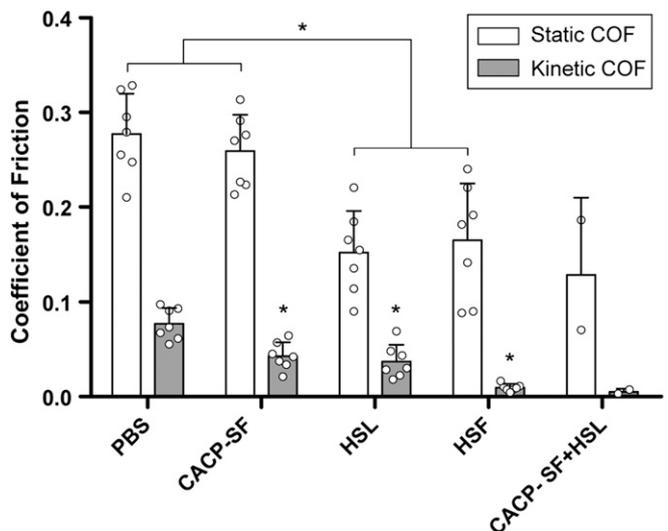

Fig. 2. COF in bovine cartilage bearings lubricated with different test solutions. Bar graphs depicting mean + 1 SD static (unshaded) and kinetic (shaded) COF measurements in bovine cartilage bearings lubricated with either PBS, SF from patients with CACP (CACP-SF), purified human synoviocyte lubricin (HSL), human synovial fluid from normal joints (HSF), and CACP-SF that has been supplemented with HSL (CACP-SF+HSL). Static COF was significantly higher in PBS and CACP-SF lubricated bearings compared with HSL- and HSF-lubricated bearings. Kinetic COF was significantly higher in bearings lubricated with PBS compared with all other groups.
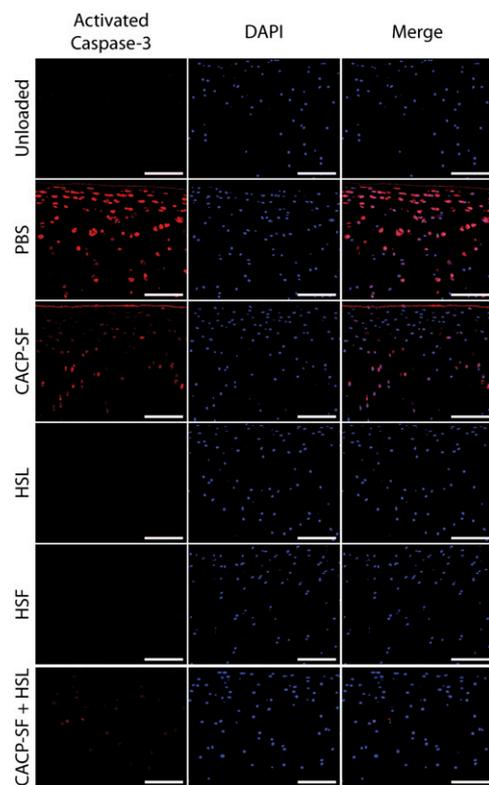
Fig. 3. Apoptosis in bovine cartilage bearings lubricated with different test solutions. The lower explant cartilage bearings were stained for active caspase-3 (red, left column), and nuclei were counterstained with DAPI (blue, middle column) following friction and wear testing. Images were merged to show colocalization of caspase-3 within cells (right column). We observed many apoptotic cells in the superficial and upper middle zones of PBS and CACP-SF–lubricated samples, whereas few apoptotic cells were observed in the unloaded bearings and in bearings lubricated with HSL, HSF, or CACP-SF + HSL. (Scale bars, 100 μm.)

Bearings tested with PBS and CACP-SF had higher mean percentages of apoptotic chondrocytes in the top and middle layers, compared with HSF- and HSL-lubricated bearings and to unloaded bearings (Fig. 4*B*). In addition, the more superficial layer of bearings tested with PBS and CACP-SF contained a greater percentage of apoptotic chondrocytes compared with the next layer. For example, in CACP-SF–lubricated bearings, the percentage of apoptotic cells in the top layer (zone A) was greater than that of the middle layer ($P < 0.001$) and the middle layer (zone B) was greater than that of the lower layer (zone C) ($P = 0.015$).

Finally, when we graphed static COF and percentage of apoptotic chondrocytes in superficial zone (top layer) independent of the supplemented lubricant, we found a significant correlation between friction and cell death ($r^2 = 0.41$, $P = 0.0007$) (Fig. 4*C*).

Discussion

Herein, we show that increasing static friction causes the death of superficial and upper intermediate zone chondrocytes. SF from CACP donors in a cartilage-on-cartilage bearing system failed to reduce static friction and increased chondrocyte apoptosis compared with normal HSF or purified human lubricin. In addition, $Prg4^{-/-}$ mouse knees had more apoptotic cells and higher whole-joint COF compared with $Prg4^{+/+}$ and $Prg4^{+/-}$ knees. These results support the hypothesis that increased friction in an articular joint causes chondrocyte apoptosis, which results in progressive loss of extracellular matrix and ultimately joint failure. Consistent with earlier studies (13, 20, 22, 23, 26–

29), our study confirms the importance of lubricin in providing boundary lubrication to preserve structural and cellular integrity at the cartilage surface.

Boundary lubrication decreases friction between surface asperities that are pressurized together during periods of high load and low speed (30). This paradigm is particularly relevant in large weight-bearing joints, when the fluid layer normally found on the surface of cartilage is measurably thinner than surface asperities (16, 30, 31). In this study, the axial load is held constant across samples, testing the ability of each test solution to provide boundary lubrication, prevent shear stress, resultant strain, and consequential chondrocyte apoptosis. Lack of boundary lubrication causes stick-slip to occur, which results in subsurface strain (32) and causes surface asperities to deform destructively (24, 33). In contrast to the inability of CACP-SF to reduce static COF, CACP-SF had the same ability to lower kinetic COF as purified human lubricin, yet this reduction in kinetic COF did not prevent apoptosis. It should be noted that kinetic COF values may represent contributions of both mixed mode and boundary modes of lubrication. Therefore, the chondroprotective properties of lubricin are linked to its ability to lower COF at the initiation of motion. Further support for this mechanism derives from the observation that adding purified HSL to CACP-SF restored the fluid's ability to lower static COF and to prevent apoptosis.

Pendulum analysis allows the observation of contributions of adherent sliding surfaces that naturally articulate in a roller–slider movement. Elevated whole-joint COF in $Prg4^{-/-}$ mouse joints is directly related to the absence of lubricin in SF and may also be influenced by cartilage surface damage and protein deposition that characterize the $Prg4^{-/-}$ phenotype. Interestingly, in our mouse limbs and in the bovine cartilage bearing model, when lubricin was missing, the occurrence of chondrocyte apoptosis was greatest just below the cartilage surface (Figs. 1*A* and 3). Previous work looking at shear deformation and shear strain in cartilage explants from human (32, 34) and neonatal bovine (34, 35) sources found shear deformation was highest in the uppermost layers of cartilage, just below the superficial zone, and did not propagate linearly. Furthermore, under 10% compressive axial strain, cartilage explants experienced the largest deformations in the transitional region between the superficial and intermediate zone (34). Our finding of increased chondrocyte apoptosis at these locations when lubricin is missing is consistent with the predicted sites of maximum tissue deformation, especially around cells just below the superficial zone (35). Previous studies have reported elevated shear strain and cartilage deformation in human cartilage explants when lubricated with PBS as opposed to normal bovine SF (32). Furthermore, shear strain is exaggerated in degenerative cartilage samples (32). Also of interest are reports that administering pancaspase inhibitors to experimental OA models resulted in fewer cartilage lesions by preventing cell death (8, 36).

Lubricin is normally produced in synovial joints by synovial fibroblasts and superficial zone chondrocytes. Shear stress and compression increase lubricin expression in bovine cartilage when lubricated (37, 38), so the viability of lubricin-producing cells in the superficial zone and the availability of lubricin in SF to deposit on the cartilage surface help maintain boundary lubrication (39). The importance of rapid and continuous replenishment of lubricin during joint loading is supported by our studies, which found a significant increase in COF after 30 h of ex vivo joint oscillation under load in $Prg4^{+/-}$ compared with $Prg4^{+/+}$ mouse limbs (22). $Prg4^{+/-}$ limbs do not exhibit increased COF compared with $Prg4^{+/+}$ limbs in the absence of continuous oscillation.

In a previously normal joint, changes in lubricin abundance following injury may affect the risk for developing cartilage damage. Common traumatic knee injuries, such as anterior cruciate ligament tears, are strong risk factors for the development of
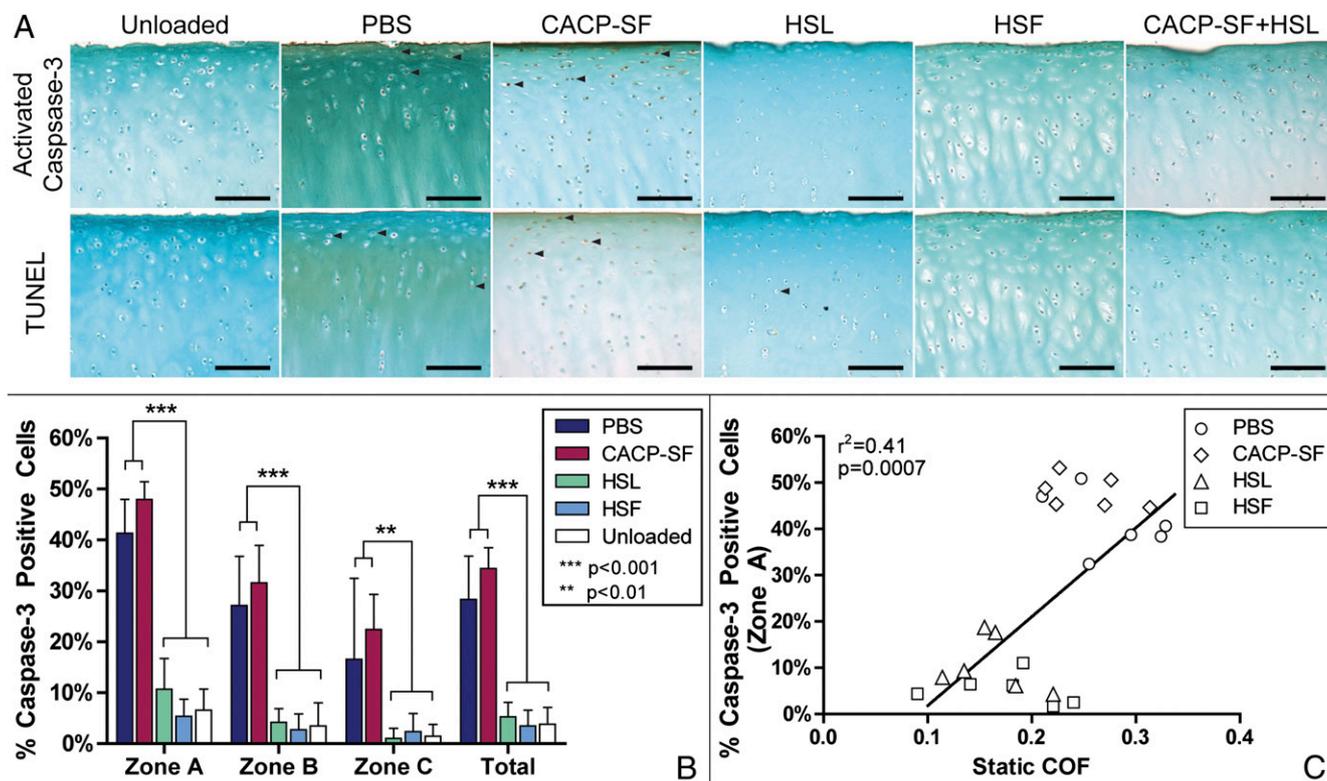
Fig. 4. (*A*) Apoptosis in lower bovine cartilage bearings analyzed by zone. Cartilage explant bearings tested with PBS and CACP-SF had a greater number of cells positive for activated caspase-3 (brown, arrowheads) than bearings lubricated with HSL, HSF, or CACP-SF+HSL and unloaded bearings. Cells negative for activated caspase-3 are stained blue. TUNEL staining (brown) confirmed apoptosis in bearings lubricated with PBS and CACP-SF (arrowheads), but few cells were TUNEL positive in the bearings lubricated with HSL, HSF, or CACP-SF+HSL or in unloaded bearings. Cells negative for TUNEL are stained blue. (Scale bars, 100 μm.) (*B*) Percentage of activated caspase-3 in lower bovine cartilage bearings. Bearings tested with PBS and CACP-SF had significantly higher percentages of apoptotic cells in the superficial and upper middle zones compared with unloaded bearings and bearings lubricated with HSL and HSF. Error bars indicate SD. (*C*) Correlation of static COF and activated caspase-3 in zone A. A significant correlation ($r^2 = 0.41$) between static COF and activated caspase-3–positive cells in zone A (articular surface, 100 μm) was observed for the mechanically tested bearings, across the different lubricants.

OA. Lubricin levels in SF decrease after anterior cruciate ligament injury and can take up to a year to return to baseline values (40). Several studies have demonstrated a disease-modifying effect for the intraarticular injection of native or recombinantly expressed lubricin in rodent models of posttraumatic OA (28, 29, 41, 42). Our data indicate that lubricin supplementation likely protects damaged joints by preserving boundary lubrication, thereby protecting articular chondrocytes from apoptosis caused by excessive deformation and shear stress.

Due to the ability of lubricin to reestablish boundary lubrication, provide chondroprotection and restore a low COF in the boundary mode, this study suggests that lubricin could be used as a therapy in patients with transient deficiency of lubricin, as can occur following traumatic joint injury or inflammatory joint disease. Additional work introducing lubricin in lubricin-null mice through intraarticular injection may provide the basis for a future clinical study in patients with CACP, or in patients with acquired arthropathy.

Materials and Methods

Modified Stanton Pendulum. Hindlimbs were excised from *Prg4*$^{-/-}$ (*n* = 6 limbs, *n* = 5 mice), *Prg4*$^{+/-}$ (*n* = 6 limbs, *n* = 5 mice), and *Prg4*$^{+/+}$ (*n* = 12 limbs, *n* = 8 mice) male, 10 ± 1-wk-old mice and tested on a modified Stanton pendulum immediately following harvest to achieve a measure of COF, as previously described (22, 43). The hindlimbs were dissected, leaving the joint capsule intact, and the proximal femur and distal tibia were rigidly embedded in square brass tubing (6.25 mm wide) using a urethane potting compound (Smooth-ON). The pendulum arm was fitted to the tube encasing the femur, and the tube encasing the tibia was fixed to the pendulum base

using set screws, with the knee at a resting angle of 70°, which was chosen based on previous studies regarding the mean flexion angle during normal murine ambulation (44, 45). Four reflective markers were attached to the pendulum arm and four were attached to the base. Following a static loading time of 8 min where the knee was loaded with the weight of the pendulum (50 g, approximately two times body weight) and submerged in a well filled with PBS. Following the loading period, PBS was removed from the well, and the pendulum arm was rotated to a flexion angle of ~12° and released, allowing the joint to oscillate freely until motion was finished. Four trials were collected for each knee. Motion was tracked with a Qualisys AB system at a rate of 60 Hz. Oscillation data were processed with Visual3D software (C-Motion), and a custom MATLAB (MathWorks) code was used to determine the peak amplitude of each cycle of oscillation and calculate whole-joint COF using a linear Stanton linear decay model (43). The generation of these mice has been previously described and they have been backcrossed onto a C57BL6/J background strain (14). All animal research was approved by the Rhode Island Hospital Animal Welfare Committee.

Bovine Cartilage Preparation. Full-thickness cartilage plug bearings 6 and 12 mm in diameter were cored from the femoral condyle of bovine knees (*n* = 10) collected within 2 h of slaughter. Following harvest, the bearings were rinsed with cell culture media [DMEM supplemented with 5% (vol/vol) FBS] and cultured for 24 h at 37 °C.

Test Solutions. PBS (1×) was purchased from Life Technologies. HSF was aspirated from the uninjured contralateral joints of patients with an anterior cruciate ligament injury (*n* = 4). These samples were obtained without lavage just before reconstructive surgery (40). Other HSFs were aspirated from knee joints of postmortem donors with no OA within 12 h of death (two male donors; ages, 29 and 39; National Disease Research Interchange). The samples were inspected for blood contamination, and then centrifuged following aspiration at 12,000 × *g* at 4 °C for 10 min, and the aliquot was

removed and stored at −80 °C until testing. Lyophilized HSL was obtained from SBH Sciences and has been characterized previously (41, 42). This product was solubilized using distilled water to a concentration of 250 µg/mL, which is the estimated lubricin concentration in SF (40). SF from patients with CACP (CACP-SF) was obtained from patients in the years between 2000 and 2011, following diagnostic knee joint aspiration (*n* = 4). CACP-SF samples were inspected for blood contamination, and then centrifuged at 12,000 × *g* at 4 °C for 10 min and stored frozen at −20 °C until testing. Lyophilized HSL was solubilized in CACP-SF (CACP+HSL) at 250 µg/mL 24 h before testing, and stored overnight at 4 °C. All lubricants were thawed to room temperature immediately before testing. Approval to obtain SF from patients was granted by the Rhode Island Hospital and Boston Children's Hospital Institutional Review Boards. Informed consent was obtained from patients.

Bovine Bearings Friction and Wear Testing. This testing method has been described previously (23). Briefly, the average total cartilage thickness for each bearing pair was calculated (2.95 ± 0.47 mm) using caliper measurements in four regions along the circumference before testing. The upper disk diameter (5.62 ± 0.47 mm) was also measured using two caliper measurements. Cartilage bearings were loaded in a disk-on-disk configuration (the lower disk diameter was 12 mm) into an EnduraTEC ElectroForce 3200 (Bose Corporation, ElectroForce Systems Group) with cyanoacrylate glue, and any remaining cell culture medium was rinsed off three times with 1-mL washes of PBS. Test lubricant was applied between the surfaces. The bearings were axially loaded to 18% total cartilage thickness, reaching a maximum load of 6.87 ± 3.6 N, and held at this displacement for 8 min to allow for fluid depressurization (25, 46). Then, the lower bearing was rotated in torsion +2 revolutions and reset −2 revolutions at an effective velocity of 0.3 mm/s, which allows the depressurized cartilage–cartilage interface to remain in the boundary mode of lubrication (25), for 12 continuous cycles. Immediately following testing, lower discs were fixed in formalin. Unloaded control discs, also 12 mm in diameter, were fixed at the time of testing. All tests were performed between 48 and 72 h of cartilage harvest, and bearings were only tested once.

Static and kinetic COFs were calculated using Eq. **1** (23):

$$COF = |Torque|/(1/3 \times Upper\ Bearing\ Diameter \times Axial\ Force). \quad \textbf{[1]}$$

To calculate static COF, the absolute maximum value of torque at the initiation of motion was used. To calculate kinetic COF, the average torque, observed during the last 720° of rotation was used. The equilibrium axial force (1.55 ± 0.82 N), which was incurred following the 8-min depressurization period, and the measured diameter of the upper bearing were used for both measurements (23).

Activated Caspase-3 Staining and Quantification. Mouse knees representing each *Prg4* genotype that were not used to measure COF and bovine femoral cartilage lower bearings that were used to measure COF were processed for active caspase-3 detection. Samples were fixed in 10% formalin and decalcified using a solution of 0.48 M EDTA adjusted pH to 7.1 with ammonium hydroxide at 4 °C for 48 h (mouse knees) or 2 wk (cartilage bearings). Thin coronal sections (6 µm) were taken for histological analysis of apoptosis of chondrocytes in the femoral condyles and tibial plateaus of mouse limbs, and full-thickness sections of large bovine bearings. Sections were heated to 60 °C for 30 min, deparaffinized, and hydrated in three changes of xylene and serial alcohol. Sections were then quenched in endogenous peroxidase in 3% hydrogen peroxide for 10 min, and antigen retrieval was performed using a pepsin solution (Thermo Scientific). A rabbit polyclonal antibody

against active caspase-3 (ab13847; Abcam) at 1:50 dilution was added to the sections and incubated at 4 °C overnight. After three washes with PBS, the sections were incubated with Cy3 goat anti-rabbit IgG (Life Technologies, Molecular Probes) at 1:50 dilution for 1 h at room temperature, protected from light. The sections were washed five times using PBS, counterstained using Vectashield mounting media with DAPI (1.5 µg/mL; Vector Laboratories). Images were captured with a 10× objective, using a Roeper Scientific Photometrics CoolSNAP HQ2 monochrome camera (Roeper Scientific) and a Nikon Eclipse 90i microscope (Nikon). Fluorescent images were thresholded uniformly to reduce background autofluorescence and to adjust DAPI signal using Adobe Photoshop CS5 software (Adobe Systems). Active caspase-3 was also immunodetected with ab13847 (Abcam) and detected using the Vectastain ABC kit (Vector Laboratories). Sections were then counterstained with 0.5% methyl green.

The percentage of apoptotic cells in bovine sections was determined using images captured at 20× with Image-Pro Plus software (Media Cyberkinetics). The number of active caspase-3–positive cells was divided by the total number of cell nuclei in three 100-µm-thick cartilage layers beginning at the cartilage surface. The total percentage of apoptotic cells was the mean across all three zones.

TUNEL Staining. We used the ApopTag Plus Peroxidase In Situ Apoptosis Kit (Millipore). Mouse knee and bovine cartilage bearing samples were fixed, decalcified, and embedded as previously described (23). Sections were heated at 60 °C for 30 min and deparaffinized in three changes of xylene and serial ethanol. Then, sections were pretreated with proteinase K (20 µg/mL) for 15 min at room temperature, quenched with endogenous peroxidase in 3% hydrogen peroxide for 5 min, and incubated with equilibration buffer for 30 s. Sections were treated with terminal deoxynucleotidyltransferase enzyme at 37 °C for 1 h in a humidified chamber, washed three times in PBS, incubated with anti-digoxigenin conjugate for 30 min at room temperature, and washed in PBS. Peroxidase substrate was applied to sections, which were stained for 4 min, washed in deionized water, and counterstained with 0.5% methyl green. Sections were washed in deionized water again, dehydrated in xylene three times, and then mounted with Permount mounting media. Images were captured at 20× with Image-Pro Plus software.

Statistical Analysis. Statistical analysis was performed using a one-way ANOVA on ranks (α ≤ 0.05) with Dunn's comparison tests for COF in *Prg4* mouse limbs. Statistical analysis for bovine bearing static and kinetic COF between groups lubricated with different test lubricants was performed using a one-way ANOVA with Holm–Sidak multiple comparison post hoc tests. A Student's *t* test was used to determine the difference between the static COF of bearings lubricated with CACP-SF and CACP-SF+HSL. Linear regression analysis was performed comparing static COF and the percentage of activated caspase-3–positive cells in the top 100-µm layer. Differences between apoptosis in the three zones of bovine cartilage discs were analyzed using a two-way repeated-measures ANOVA (α ≤ 0.05) with Holm–Sidak multiple-comparison post hoc tests, using SigmaPlot software (Systat Software). All other statistics were performed using Prism 6 Statistical Software (GraphPad Software), and all values are reported as mean ± SD.

1. Yang KGA, Saris DBF, Dhert WJA, Verbout AJ (2004) Osteoarthritis of the knee: Current treatment options and future directions. *Curr Orthop* 18(4):311–320.
2. Jay GD (2004) Lubricin and surfacing of articular joints. *Curr Opin Orthop* 15(5):355–359.
3. Lorenz H, Richter W (2006) Osteoarthritis: Cellular and molecular changes in degenerating cartilage. *Prog Histochem Cytochem* 40(3):135–163.
4. Goggs R, Carter SD, Schulze-Tanzil G, Shakibaei M, Mobasheri A (2003) Apoptosis and the loss of chondrocyte survival signals contribute to articular cartilage degradation in osteoarthritis. *Vet J* 166(2):140–158.
5. Goldring MB (2000) The role of the chondrocyte in osteoarthritis. *Arthritis Rheum* 43(9):1916–1926.
6. Kühn K, D'Lima DD, Hashimoto S, Lotz M (2004) Cell death in cartilage. *Osteoarthritis Cartilage* 12(1):1–16.
7. Thomas CM, Fuller CJ, Whittles CE, Sharif M (2007) Chondrocyte death by apoptosis is associated with cartilage matrix degradation. *Osteoarthritis Cartilage* 15(1):27–34.
8. D'Lima D, Hermida J, Hashimoto S, Colwell C, Lotz M (2006) Caspase inhibitors reduce severity of cartilage lesions in experimental osteoarthritis. *Arthritis Rheum* 54(6):1814–1821.
9. Blanco FJ, Guitian R, Vázquez-Martul E, de Toro FJ, Galdo F (1998) Osteoarthritis chondrocytes die by apoptosis. A possible pathway for osteoarthritis pathology. *Arthritis Rheum* 41(2):284–289.
10. Sharif M, Whitehouse A, Sharman P, Perry M, Adams M (2004) Increased apoptosis in human osteoarthritic cartilage corresponds to reduced cell density and expression of caspase-3. *Arthritis Rheum* 50(2):507–515.
11. Flannery CR, et al. (1999) Articular cartilage superficial zone protein (SZP) is homologous to megakaryocyte stimulating factor precursor and Is a multifunctional proteoglycan with potential growth-promoting, cytoprotective, and lubricating properties in cartilage metabolism. *Biochem Biophys Res Commun* 254(3):535–541.
12. Jay GD, Lane BP, Sokoloff L (1992) Characterization of a bovine synovial fluid lubricating factor. III. The interaction with hyaluronic acid. *Connect Tissue Res* 28(4):245–255.
13. Greene GW, et al. (2011) Adaptive mechanically controlled lubrication mechanism found in articular joints. *Proc Natl Acad Sci USA* 108(13):5255–5259.
14. Rhee DK, et al. (2005) The secreted glycoprotein lubricin protects cartilage surfaces and inhibits synovial cell overgrowth. *J Clin Invest* 115(3):622–631.

15. Jay GD, Britt DE, Cha CJ (2000) Lubricin is a product of megakaryocyte stimulating factor gene expression by human synovial fibroblasts. *J Rheumatol* 27(3):594–600.

16. Yakubov GE, McColl J, Bongaerts JH, Ramsden JJ (2009) Viscous boundary lubrication of hydrophobic surfaces by mucin. *Langmuir* 25(4):2313–2321.

17. Swann DA, Sotman S, Dixon M, Brooks C (1977) The isolation and partial characterization of the major glycoprotein (LGP-I) from the articular lubricating fraction from bovine synovial fluid. *Biochem J* 161(3):473–485.

18. Coles JM, et al. (2010) Loss of cartilage structure, stiffness, and frictional properties in mice lacking PRG4. *Arthritis Rheum* 62(6):1666–1674.

19. Jay GD, Harris DA, Cha CJ (2001) Boundary lubrication by lubricin is mediated by O-linked beta(1-3)Gal-GalNAc oligosaccharides. *Glycoconj J* 18(10):807–815.

20. Zappone B, Ruths M, Greene GW, Jay GD, Israelachvili JN (2007) Adsorption, lubrication, and wear of lubricin on model surfaces: Polymer brush-like behavior of a glycoprotein. *Biophys J* 92(5):1693–1708.

21. Marcelino J, et al. (1999) CACP, encoding a secreted proteoglycan, is mutated in camptodactyly-arthropathy-coxa vara-pericarditis syndrome. *Nat Genet* 23(3):319–322.

22. Drewniak EI, et al. (2012) Cyclic loading increases friction and changes cartilage surface integrity in lubricin-mutant mouse knees. *Arthritis Rheum* 64(2):465–473.

23. Waller KA, Zhang LX, Fleming BC, Jay GD (2012) Preventing friction-induced chondrocyte apoptosis: Comparison of human synovial fluid and hylan G-F 20. *J Rheumatol* 39(7):1473–1480.

24. Jay GD, et al. (2007) Association between friction and wear in diarthrodial joints lacking lubricin. *Arthritis Rheum* 56(11):3662–3669.

25. Schmidt TA, Gastelum NS, Nguyen QT, Schumacher BL, Sah RL (2007) Boundary lubrication of articular cartilage: Role of synovial fluid constituents. *Arthritis Rheum* 56(3):882–891.

26. Teeple E, et al. (2008) Coefficients of friction, lubricin, and cartilage damage in the anterior cruciate ligament-deficient guinea pig knee. *J Orthop Res* 26(2):231–237.

27. Jones AR, Flannery CR (2007) Bioregulation of lubricin expression by growth factors and cytokines. *Eur Cell Mater* 13:40–45, discussion 45.

28. Elsaid KA, et al. (2012) The impact of forced joint exercise on lubricin biosynthesis from articular cartilage following ACL transection and intra-articular lubricin's effect in exercised joints following ACL transection. *Osteoarthritis Cartilage* 20(8):940–948.

29. Flannery CR, et al. (2009) Prevention of cartilage degeneration in a rat model of osteoarthritis by intraarticular treatment with recombinant lubricin. *Arthritis Rheum* 60(3):840–847.

30. Gleghorn JP, Bonassar LJ (2008) Lubrication mode analysis of articular cartilage using Stribeck surfaces. *J Biomech* 41(9):1910–1918.

31. Coles JM, Chang DP, Zauscher S (2010) Molecular mechanisms of aqueous boundary lubrication by mucinous glycoproteins. *Curr Opin Colloid Interface Sci* 15(6):406–416.

32. Wong BL, Bae WC, Gratz KR, Sah RL (2008) Shear deformation kinematics during cartilage articulation: Effect of lubrication, degeneration, and stress relaxation. *Mol Cell Biomech* 5(3):197–206.

33. Chan SM, Neu CP, Komvopoulos K, Reddi AH (2011) Dependence of nanoscale friction and adhesion properties of articular cartilage on contact load. *J Biomech* 44(7):1340–1345.

34. Buckley MR, Bergou AJ, Fouchard J, Bonassar LJ, Cohen I (2010) High-resolution spatial mapping of shear properties in cartilage. *J Biomech* 43(4):796–800.

35. Buckley MR, Gleghorn JP, Bonassar LJ, Cohen I (2008) Mapping the depth dependence of shear properties in articular cartilage. *J Biomech* 41(11):2430–2437.

36. Dang AC, Warren AP, Kim HT (2006) Beneficial effects of intra-articular caspase inhibition therapy following osteochondral injury. *Osteoarthritis Cartilage* 14(6):526–532.

37. Nugent GE, et al. (2006) Dynamic shear stimulation of bovine cartilage biosynthesis of proteoglycan 4. *Arthritis Rheum* 54(6):1888–1896.

38. Nugent GE, et al. (2006) Static and dynamic compression regulate cartilage metabolism of PRoteoGlycan 4 (PRG4). *Biorheology* 43(3–4):191–200.

39. Chan SM, Neu CP, DuRaine G, Komvopoulos K, Reddi AH (2012) Tribological altruism: A sacrificial layer mechanism of synovial joint lubrication in articular cartilage. *J Biomech* 45(14):2426–2431.

40. Elsaid KA, et al. (2008) Decreased lubricin concentrations and markers of joint inflammation in the synovial fluid of patients with anterior cruciate ligament injury. *Arthritis Rheum* 58(6):1707–1715.

41. Jay GD, et al. (2010) Prevention of cartilage degeneration and restoration of chondroprotection by lubricin tribosupplementation in the rat following anterior cruciate ligament transection. *Arthritis Rheum* 62(8):2382–2391.

42. Jay GD, et al. (2012) Prevention of cartilage degeneration and gait asymmetry by lubricin tribosupplementation in the rat following anterior cruciate ligament transection. *Arthritis Rheum* 64(4):1162–1171.

43. Drewniak EI, Jay GD, Fleming BC, Crisco JJ (2009) Comparison of two methods for calculating the frictional properties of articular cartilage using a simple pendulum and intact mouse knee joints. *J Biomech* 42(12):1996–1999.

44. Fischer MS, Schilling N, Schmidt M, Haarhaus D, Witte H (2002) Basic limb kinematics of small therian mammals. *J Exp Biol* 205(Pt 9):1315–1338.

45. Fischer MS, Blickhan R (2006) The tri-segmented limbs of therian mammals: Kinematics, dynamics, and self-stabilization–a review. *J Exp Zoolog A Comp Exp Biol* 305(11):935–952.

46. Park S, Costa KD, Ateshian GA (2004) Microscale frictional response of bovine articular cartilage from atomic force microscopy. *J Biomech* 37(11):1679–1687.